



ARL-TR-9364 • DEC 2021



Evaluation of Local Thickness and the Lineal Intercept Method as Grain Size Metrics

by Bobby C Kaman, Daniel O Lewis, James D Paramore, and
Brady G Butler

Approved for public release: distribution unlimited.

NOTICE

Disclaimers

The findings in this report are not to be construed as an official Department of the Army position unless so designated by other authorized documents.

Citation of manufacturer's or trade names does not constitute an official endorsement or approval of the use thereof.

Destroy this report when it is no longer needed. Do not return it to the originator.



Evaluation of Local Thickness and the Lineal Intercept Method as Grain Size Metrics

James D Paramore and Brady G Butler
Weapons and Materials Research Directorate
DEVCOM Army Research Laboratory

Bobby C Kaman
Iowa State University

Daniel O Lewis
Texas A&M University

REPORT DOCUMENTATION PAGE

Form Approved
OMB No. 0704-0188

Public reporting burden for this collection of information is estimated to average 1 hour per response, including the time for reviewing instructions, searching existing data sources, gathering and maintaining the data needed, and completing and reviewing the collection information. Send comments regarding this burden estimate or any other aspect of this collection of information, including suggestions for reducing the burden, to Department of Defense, Washington Headquarters Services, Directorate for Information Operations and Reports (0704-0188), 1215 Jefferson Davis Highway, Suite 1204, Arlington, VA 22202-4302. Respondents should be aware that notwithstanding any other provision of law, no person shall be subject to any penalty for failing to comply with a collection of information if it does not display a currently valid OMB control number.

PLEASE DO NOT RETURN YOUR FORM TO THE ABOVE ADDRESS.

1. REPORT DATE (DD-MM-YYYY) December 2021		2. REPORT TYPE Technical Report		3. DATES COVERED (From - To) 26 May–3 August 2021	
4. TITLE AND SUBTITLE Evaluation of Local Thickness and the Lineal Intercept Method as Grain Size Metrics				5a. CONTRACT NUMBER W911NF-19-2-0264	
				5b. GRANT NUMBER	
				5c. PROGRAM ELEMENT NUMBER	
6. AUTHOR(S) Bobby C Kaman, Daniel O Lewis, James D Paramore, and Brady G Butler				5d. PROJECT NUMBER	
				5e. TASK NUMBER	
				5f. WORK UNIT NUMBER	
7. PERFORMING ORGANIZATION NAME(S) AND ADDRESS(ES) DEVCOM Army Research Laboratory ATTN: FCDD-RLW-MF Aberdeen Proving Ground, MD 21005				8. PERFORMING ORGANIZATION REPORT NUMBER ARL-TR-9364	
9. SPONSORING/MONITORING AGENCY NAME(S) AND ADDRESS(ES)				10. SPONSOR/MONITOR'S ACRONYM(S)	
				11. SPONSOR/MONITOR'S REPORT NUMBER(S)	
12. DISTRIBUTION/AVAILABILITY STATEMENT Approved for public release: distribution unlimited.					
13. SUPPLEMENTARY NOTES ORCID IDs: Brady Butler, 0000-0002-7677-9685; James Paramore, 0000-0001-8058-7662					
14. ABSTRACT Microstructure analysis is an essential part of any attempt to describe a material; many engineering materials' particular properties can be attributed their specific microstructural features rather than their bulk composition. Grain size distributions and their centrality measurements are commonly used to describe the scale of microstructural features. The lineal intercept method is a standard grain-size metric that returns either a mean grain size or grain size distribution (depending on the specific application of the method). Here, this method is compared with "local thickness" distributions of a microstructure. This distribution describes the size of the largest circle that can be inscribed at every pixel. It is an area-weighted measurement and describes something fundamentally different about the shapes but is found to be proportional for equiaxed microstructures. Definitions are given and strengths, weaknesses, and caveats are discussed for each method. Distributions are directly compared for single- and multi-mode grain size distributions generated from Voronoi diagrams. The sensitivity of each method to poor image segmentation is also explored.					
15. SUBJECT TERMS grain size analysis, multimodal grain size, microscopy, image segmentation, image analysis					
16. SECURITY CLASSIFICATION OF:			17. LIMITATION OF ABSTRACT UU	18. NUMBER OF PAGES 22	19a. NAME OF RESPONSIBLE PERSON Brady G Butler
a. REPORT Unclassified	b. ABSTRACT Unclassified	c. THIS PAGE Unclassified			19b. TELEPHONE NUMBER (Include area code) (410) 306-0835

Contents

List of Figures	iv
Acknowledgments	v
1. Introduction	1
2. Definitions and Methods	1
2.1 The Intercept Method	1
2.1.1 Definition	1
2.1.2 Description of Shapes	2
2.1.3 Measurement Weighting	3
2.2 Local Thickness	3
2.2.1 Definition	3
2.2.2 Description of Shapes	4
2.2.3 Measurement Weighting	5
2.3 Voronoi Tessellations	6
2.4 Simulations of Poor Segmentation	6
3. Results and Discussion	7
3.1 Descriptions of Single-Mode Microstructures	7
3.2 Descriptions of Multimodal Microstructures	8
3.3 Sensitivity to Poor Segmentation	10
4. Conclusions	11
5. Future Work	11
6. References	13
List of Symbols, Abbreviations, and Acronyms	14
Distribution List	15

List of Figures

Fig. 1	Artist’s rendering of a 2D projection of a familiar waterfowl, provided to illustrate how the function describes complex shapes. a) Original binary image. Black pixels indicate the region of interest. b) Thickness heat map. This could also be displayed as a 3D plot where a pixel’s value is its z-coordinate. Black pixels have no value (i.e., “NaN”) and are not included in the statistics.....	4
Fig. 2	Example of the thresholding of a thickness plot to determine microstructure metrics. a) A Voronoi diagram of manually placed points made to represent a multimodal grain size distribution. A thickness heatmap is overlaid and grain boundaries are highlighted. b) A thresholding to intermediate thickness values; red pixels represent selected pixels. c) A thresholding to select pixels with thickness greater than 50% of the maximum.....	5
Fig. 3	Voronoi diagrams with a) 200, b) 400, and c) 800 points per image ...	6
Fig. 4	Examples of the same micrograph after 100 iterations of each program. The goal of each program was a) adding only point-like inclusions, b) partially erasing boundaries and adding scratches, and c) erasing many boundaries and adding some point-like inclusions.....	7
Fig. 5	a) Thickness and b) lineal intercept means as a function of point density.....	7
Fig. 6	Direct comparison of metric means. Dashed lines show other possible trends.....	8
Fig. 7	a) The low-aspect-ratio structure’s thickness heat map and associated kernel density estimation (KDE) plots, and b) the high-aspect-ratio structure’s thickness heat map and associated KDE plots. Distributions’ horizontal axes are in pixels and vertical units are arbitrary.....	9
Fig. 8	Methods a, b, and c from Section 2.4 and their mean deviation plots	10

Acknowledgments

This work was supported by a cooperative agreement between DEVCOM ARL and Texas A&M University under contract number W911NF-19-2-0264. This work was supported by the US Department of Energy, National Nuclear Security Administration, under award no. DE-NA0003857.

1. Introduction

It is essential to analyze microstructural features in any attempt to describe a structural material's behavior. One of the most basic descriptions is the size of microstructural features such as grains. "Grain size", however, is not a method or a number. There are many ways it is measured, and although its true expression would be a probability distribution, it is usually described with an average of a distribution. One commonly used ASTM standard¹ describes the total number of line intercepts divided by the length of lines to provide a grain size approximation. A different method is presented here, which describes the microstructure through inscribed circles. This is a sort of brute-force, computationally intensive method that involves making measurements at every pixel. However, as computational tools continue to become more powerful, brute-force methods become more practical. In all cases, these methods require analysis of subspaces of the microstructure. In fact, the traditional intercept method involves analysis of 1D subspaces. These are fundamentally different metrics of grain size and have different weightings associated with their probability distributions. The inaccuracies of each method are explored here through analysis of Voronoi tessellations modeling synthetic microstructures.

2. Definitions and Methods

Methods for image analysis and explicit definitions of two grain-size metrics are detailed in this section. For each metric, a brief qualitative explanation is given for simple shapes. Each metric describes an inherently different characteristic of the microstructure and has a distribution with different weighting.

2.1 The Intercept Method

The intercept method exists in several different forms. The form used in this study is described in the following. The analyses were conducted in MIPAR² image analysis software.

2.1.1 Definition

The size distribution was created using the following procedure. Here, "pixel" refers to a measurement of distance, rather than area, and it is equal to the side length of a pixel. Other references to the word "pixel" frequently refer to the area unit.

- 1) Randomly choose two sides of the image and randomly choose two points (one on either side).
- 2) Draw a line, with subpixel resolution, between these two points.
- 3) For each intercept this line makes through a region of selected pixels, measure the length of this segment.
 - If this length is greater than three pixels, record this as an intercept length.
 - If the length between two endpoints is less than three pixels, reject this intercept and add its length to an intercept length adjacent to it.

The subprocesses in Step 3 are implemented to remove unwanted artifacts from measurement of a pixelated image with a subpixel resolution line. This was done 10,000 times to generate the intercept length distribution.

2.1.2 Description of Shapes

This method is a variation on more-traditional methods for measuring this metric by hand. Here, individual intercept lengths are measured to generate a distribution. Traditionally, lines are drawn along a grid, and the average intercept length is measured by dividing the line length by the number of boundary intercepts.¹ This is a shortcut; it assumes zero-width boundaries and is analogous to taking averages of averages. This traditional method is not valid for two-phase materials in which boundaries of non-negligible width exist.

Because the digital method is related to this manual measurement, it is also closely related to the amount of surface area per unit volume. In fact, assuming zero-width boundaries, the expected value of a microstructure's mean lineal intercept is explicitly proportional to its surface-area-to-volume ratio.³

This is easy to visualize for a circle because of its rotational symmetry. The mean lineal intercept over all angles should be the same because of this symmetry. In other words, the size of the shadow it casts is the same for all angles. This mean lineal intercept is equal to the average intercept over all lines that can be drawn at one angle, as described by Eq. 1:

$$\langle \lambda \rangle = \frac{\int_0^r 2\sqrt{r^2 - x^2} dx}{r} = \frac{\pi}{2} r \quad (1)$$

where $\langle \lambda \rangle$ is the expected value of the mean lineal intercept, r is the radius of the circle, and x is an integration variable in the same units as r .

The “(grain) size” of a circle, as defined by Eq. 1, is in fact *smaller* than its diameter. This equation has been experimentally verified with a small error that can be attributed to the pixelation and the slightly uneven sampling of the image. In fact, the previously iterated definition of “random” lines slightly undersamples the center of the image. This can be attributed to the algorithm generating randomly oriented lines.

2.1.3 Measurement Weighting

When dealing with real microstructures, the weighting of a metric needs to be considered. Here, some grains are more frequently intercepted by random lines than others. The effect of this weighting on the intercept length distribution is not clear, but shapes with larger dimensions are more likely to be sampled. For convex shapes, the weighting of a single shape should be proportional to its average Feret (caliper) diameter over all angles because this reflects the probability that a randomly positioned and oriented line will intercept the shape. This, however, is not true of intercept distributions because the total probability of a shape being intercepted has no bearing on its individual intercept distribution.

2.2 Local Thickness

Local thickness, as defined by an ImageJ macro, is a function performed on a distance map of the region of interest. It was developed by Dougherty and Kunzelmann⁴ and is an open-source plugin.

2.2.1 Definition

Local thickness is a function performed on a binary image, returning one value per pixel. The value of each pixel is equal to the diameter of the largest circle that can be drawn within the region that includes the pixel as a point in the circle.⁴ An example of a local thickness measurement is shown in Fig. 1.

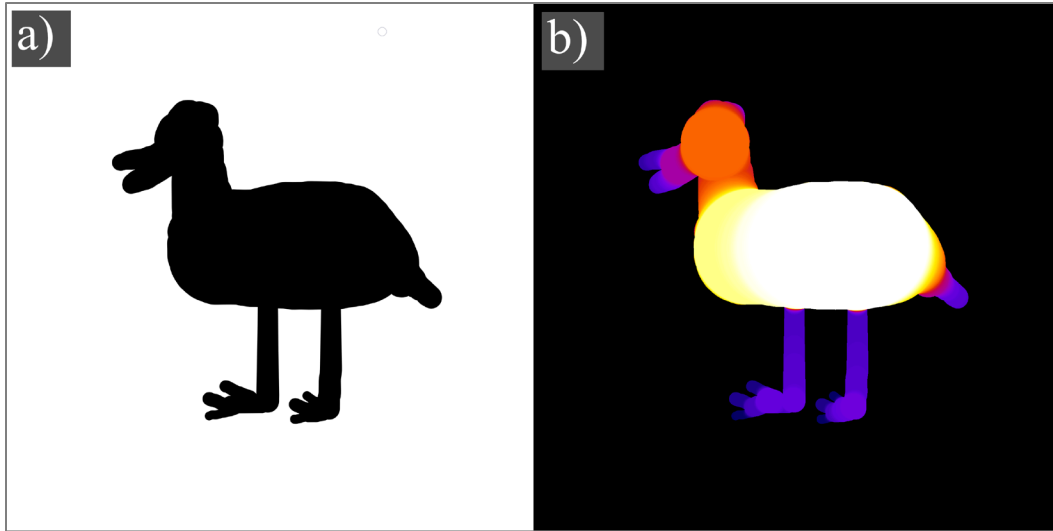


Fig. 1 Artist's rendering of a 2D projection of a familiar waterfowl, provided to illustrate how the function describes complex shapes. a) Original binary image. Black pixels indicate the region of interest. b) Thickness heat map. This could also be displayed as a 3D plot where a pixel's value is its z-coordinate. Black pixels have no value (i.e., "NaN") and are not included in the statistics.

2.2.2 Description of Shapes

This metric returns an array of values rather than a distribution (a 2D array in this instance); however, this can be done on an image stack (in which case the output would be a 3D array). A thickness distribution can be taken directly from this, or its information can be preserved and further analyzed as in Fig. 2. This allows additional information such as regional grain-size averages and volume fractions of size thresholds to be accessed easily.

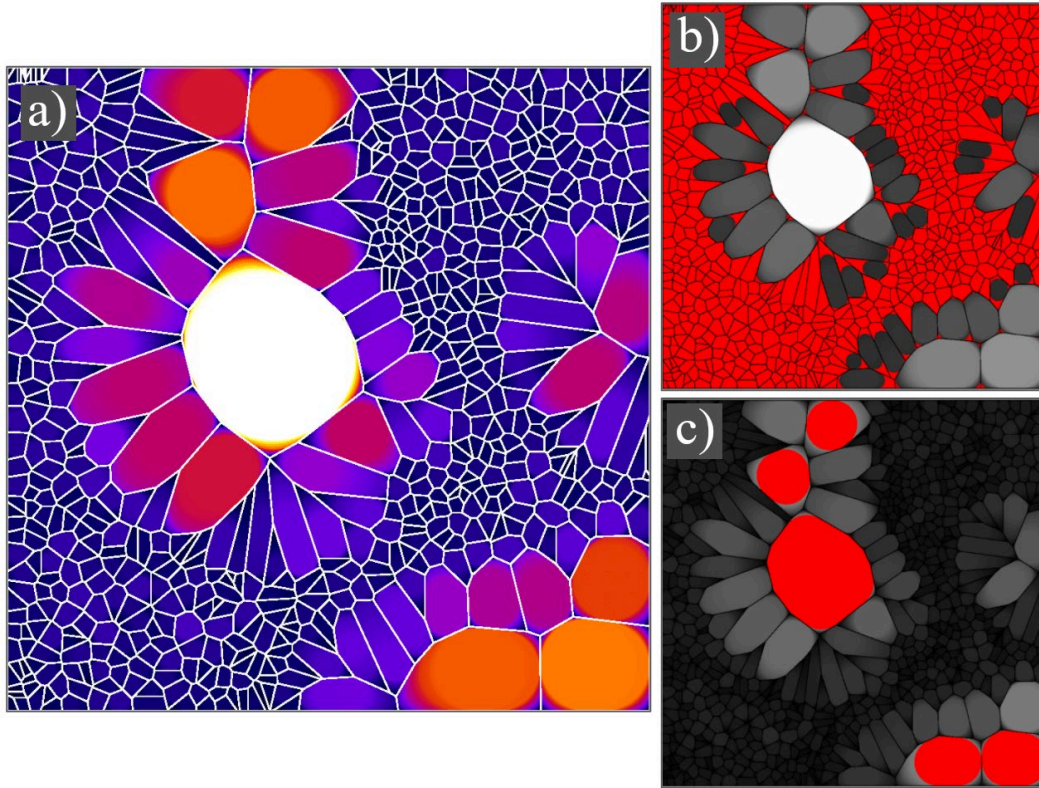


Fig. 2 Example of the thresholding of a thickness plot to determine microstructure metrics. a) A Voronoi diagram of manually placed points made to represent a multimodal grain size distribution. A thickness heatmap is overlaid and grain boundaries are highlighted. b) A thresholding to intermediate thickness values; red pixels represent selected pixels. c) A thresholding to select pixels with thickness greater than 50% of the maximum.

Note the intercept method's distribution neither truly describes grains' diameters, nor does this metric's distribution (though this is a good approximation for equiaxed grains). For many convex shapes, the thickness distribution of pixels within a grain has a large peak at the shape's minimum caliper diameter. In the case of a circle, the thickness at every pixel is equal to its diameter:

$$\langle t \rangle = 2r \quad (2)$$

where $\langle t \rangle$ is the expected value of the mean thickness over the grain and r is the radius of the circle.

2.2.3 Measurement Weighting

Because each pixel has a thickness value, this distribution is area weighted. If the grains are assumed to be spherical, a volume-weighted distribution can be approximated. A similar assumption is noted as a method for determining average grain area from mean lineal intercept in ASTM-E112.¹

2.3 Voronoi Tessellations

To create artificial microstructures that were random but consistent, Voronoi tessellations were created. A Voronoi tessellation involves drawing some number of points, often randomly, and constructing bisectors between multiple nearest-neighbor points.⁵ For a given point, the smallest area enclosed by these bisectors is said to be the point's associated Voronoi cell. These cellular structures simulate grain structures fairly well, although the energetics of boundaries are not reflected by these synthetic microstructures; far too many quadruple junctions and small-angle corners exist in these images.

To investigate the way thickness and the lineal intercept method each describe a generic microstructure, Voronoi diagrams were randomly generated. These included 20–1000 points per image in increments of 20, of which a few examples are pictured in Fig. 3. An open-source HTML tool was used for this purpose: the Voronoi Diagram Generator,⁶ which is based on the algorithms developed by Fortune.⁷ In addition, two diagrams were made with manually placed points to create multimodal microstructures. One of these is pictured in Fig. 2 in the previous section. In these cases, the microstructures included exaggerated features and are examined as a non-rigorous investigation of qualitative trends.

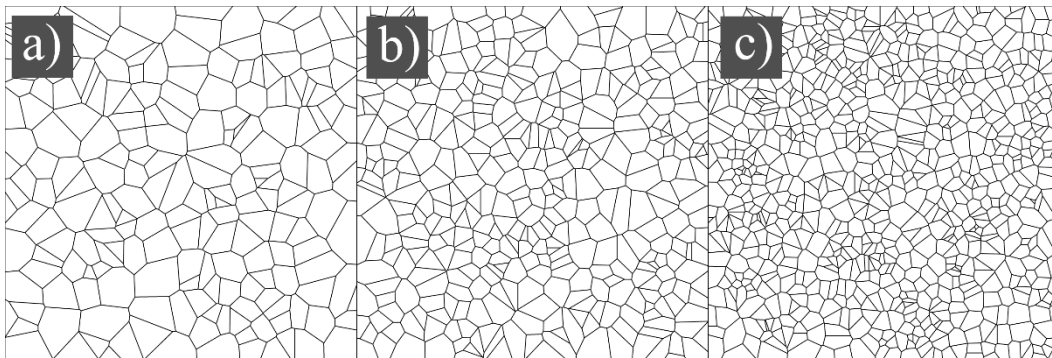


Fig. 3 Voronoi diagrams with a) 200, b) 400, and c) 800 points per image

2.4 Simulations of Poor Segmentation

To simulate the effects of poor image segmentation on each metric, three programs were written to draw black and white lines of certain thicknesses and lengths, as shown in Fig. 4. Program A was written to simulate a perfect segmentation with dark inclusions. Program B was written to include long dark lines and some incomplete boundaries, simulating a micrograph containing small but deep scratches. Program C was written to represent a poor segmentation resulting in many incomplete or missing boundaries and some dark inclusions.

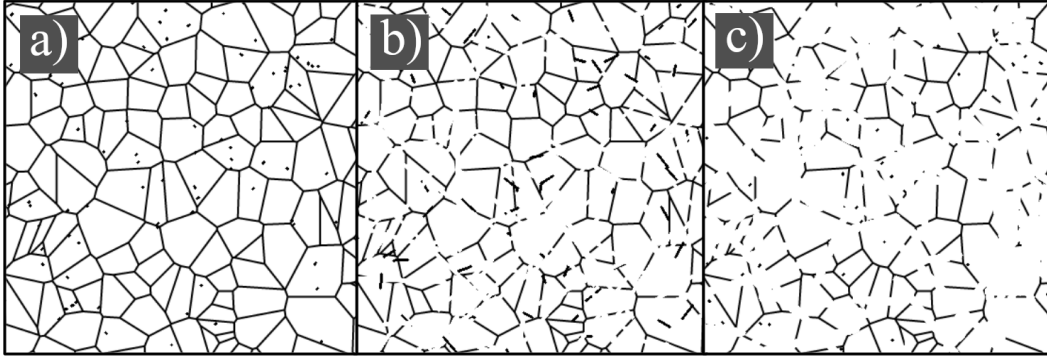


Fig. 4 Examples of the same micrograph after 100 iterations of each program. The goal of each program was a) adding only point-like inclusions, b) partially erasing boundaries and adding scratches, and c) erasing many boundaries and adding some point-like inclusions.

Each program was iterated, adding the same number of defects during each iteration. Between each iteration of a program, the image was exported for later measurement according to both methods.

3. Results and Discussion

3.1 Descriptions of Single-Mode Microstructures

Of the images with randomly generated points and varying point density, two correlations were made. Point density was compared with each metric's mean, and the means were compared across all images. The results of these analyses are shown in Fig. 5.

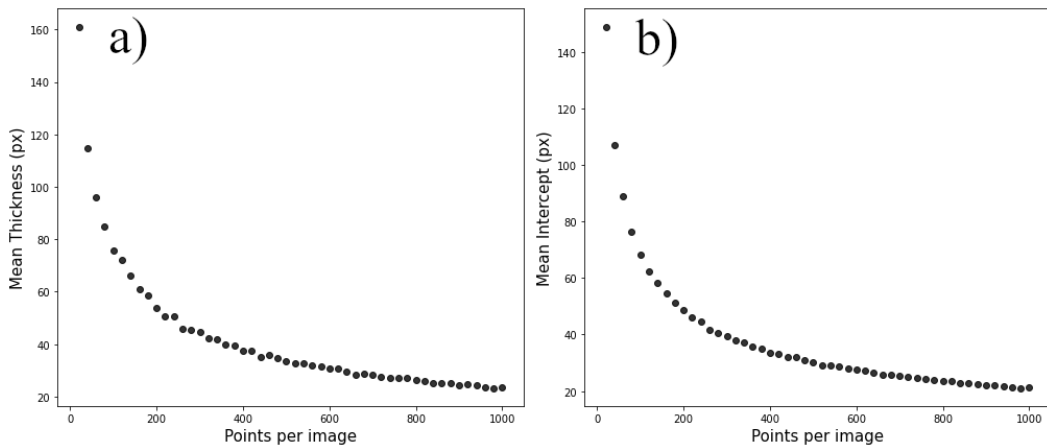


Fig. 5 a) Thickness and b) lineal intercept means as a function of point density

As could be expected, both metrics follow an inverse square relationship with point density. Unexpectedly, however, the intercept length means proved to be slightly more consistent. Both metrics appear to be good descriptors of single-mode

homogeneous microstructures, but of course they describe different things. This is illustrated by comparing the metrics' means directly (Fig. 6).

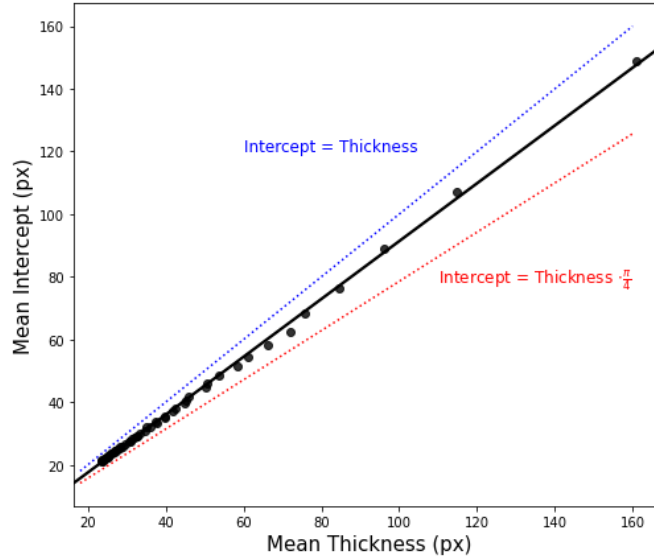


Fig. 6 Direct comparison of metric means. Dashed lines show other possible trends.

The two metrics' means follow a clear linear relationship. The slope of this line is particularly interesting—it is greater than the expected slope for a circle but less than a 1:1 correlation at approximately 0.93. In fact, it is the ratio of the mean lineal intercept to the mean thickness of the average Voronoi cell at any length scale. This ratio is characteristic of the shape of the average Voronoi cell. It is expected to depart further from circular behavior with increasing aspect ratio of the average cell.

3.2 Descriptions of Multimodal Microstructures

Manually generated Voronoi diagrams were measured with each metric to investigate the effect of varying size distribution and grain aspect ratios.

Figure 7a demonstrates the difference in the metrics as applied to a multimodal microstructure with equiaxed grains. Because local thickness is an area-weighted metric, a sharp peak is observed above 200 px. Such a peak is not observed in the intercept length distribution, though a very small one is observed around 150 px. This can be attributed to the greater weighting applied to small grains, an effect that is more exaggerated in Fig. 7b, which contains many small grains of high aspect ratio. These are more likely to be intercepted by a randomly drawn line and are therefore sampled more frequently. Because of this weighting, given only the intercept distribution, it is not obvious that the distribution has so many outliers, and the distribution looks suspiciously close to one that could fit a lognormal

probability density function. Indeed, if the log of each datum was the entry to a histogram, it would appear more similar to a skewed normal distribution than to a bimodal distribution. This is misleading; the intercept length distribution does not convey an intuitive description of the appearance of the microstructure as does the thickness distribution.

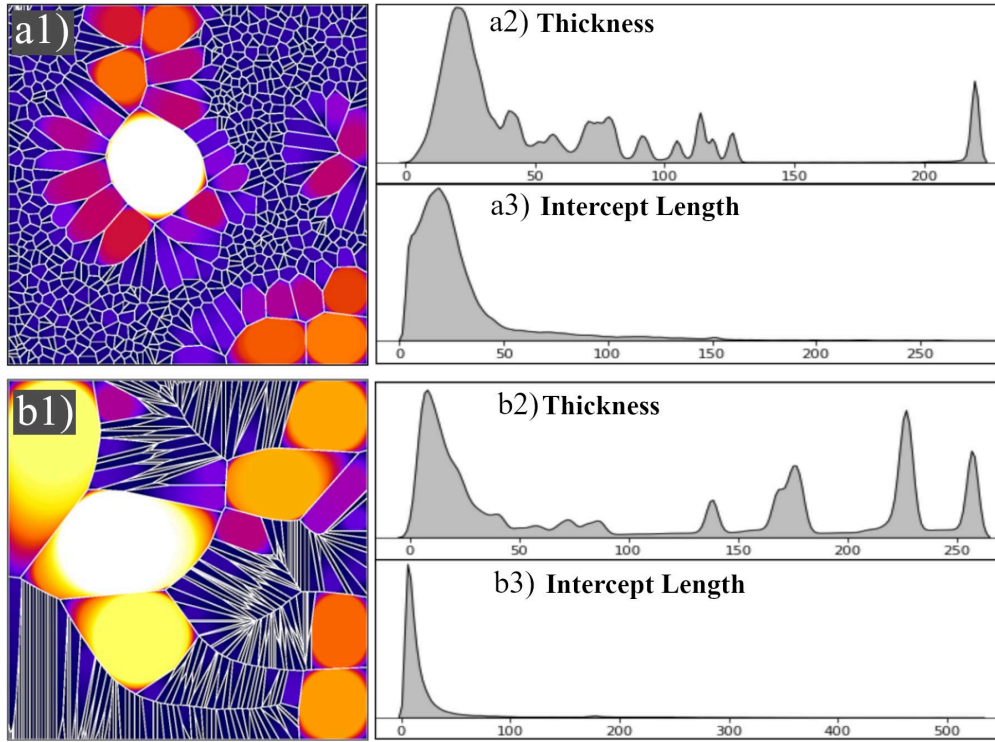


Fig. 7 a) The low-aspect-ratio structure’s thickness heat map and associated kernel density estimation (KDE) plots, and b) the high-aspect-ratio structure’s thickness heat map and associated KDE plots. Distributions’ horizontal axes are in pixels and vertical units are arbitrary.

It is nearly impossible to reconstruct a representative structure from the intercept length distribution. From the thickness distribution, however, because it is area-weighted, a group of representative shapes can be drawn. If the count in each histogram bin were divided by the square of the bin value, this new distribution would represent the number of circles that could be drawn, at each diameter, to represent the microstructure. Many small circles would be drawn that are not present in the microstructure; this is an artifact of the grains’ corners.

3.3 Sensitivity to Poor Segmentation

The three methods presented in Section 2.4 were performed, with programs being iterated between 100 and 160 times to establish trends that describe each metric's sensitivity.

The result displayed in Fig. 8a is as expected. Mean thickness is more sensitive to inclusions than mean intercept: Each dot has a small likelihood of being intercepted by a line but frequently divides larger sections of white space.

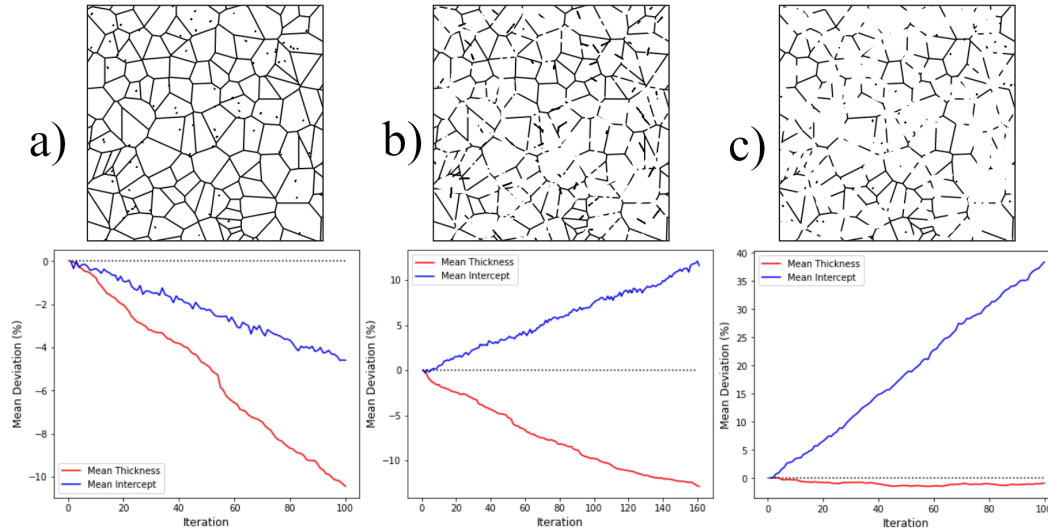


Fig. 8 Methods a, b, and c from Section 2.4 and their mean deviation plots

The result displayed in Fig. 8b is interesting. Though the result largely depends on the specifics of the algorithm, this is a result that describes these metrics well. Local thickness means are sensitive enough to inclusions that they overshadow the effect of boundary removal. Similarly, the mean lineal intercept is sensitive enough to boundary removal that it overshadows the effect of inclusions. Note that because of the aspect ratio of the inclusions (scratches), they have no small effect on the mean lineal intercept, so the effect of boundary removal is likely to be large.

The final program, Fig. 8c, simulates significant boundary removal and a few inclusions. Because the inclusions are small and boundary removal is extensive, the mean lineal intercept immediately deviates to positive values. Local thickness is primarily affected by inclusions—about twice as much as is the mean lineal intercept (pictured in Fig. 8a). However, inclusions were added less frequently and thickness is extremely insensitive to boundary removal. The result happened to balance out to a very small net deviation. The reason for this insensitivity is easy to imagine: Most grains are bound by lines, and removing a fraction of the line rarely changes the size of the largest inscribed circle that can be drawn inside the grain.

This is a particularly helpful result to know for practical purposes. If thickness is the metric of interest, an image segmentation of a microstructure has an accurate result with inaccurate (conservative) boundary detection. In many segmentations, this would present itself as a high-threshold edge-detection algorithm.

4. Conclusions

A comparison of the lineal intercept method and local thickness is presented in the context of grain size measurements. Local thickness, though non-standard, proves to be a helpful tool for describing grain size distributions accurately while preserving spatial information. It is determined that for single-mode Voronoi-like microstructures, both metrics have proportional means across length scales. Note the two metrics still describe very different things: thickness is area-weighted and the intercept method is not. For these reasons, thickness distributions appear as a more intuitive description of microstructure. However, because the function is accounting for the local thickness class at every pixel, it has the potential to be computationally intensive.

The metrics' sensitivities to poor microstructure segmentation are compared. It is evident that local thickness means are more sensitive to inclusions and very insensitive to incomplete boundaries. Mean lineal intercepts are sensitive to scratches or long inclusions and very sensitive to incomplete boundaries. In the real world, this would mean that lineal intercept may be more consistent at measuring images with large scratches, and thickness may be more consistent with images with boundaries that are difficult to distinguish.

5. Future Work

Because local thickness—as a grain size metric—preserves spatial information, this could open more experimental possibilities. It would be straightforward to conduct an experiment that measures grain size as a function of distance from some surface. This could help quantify dependencies on things like cooling rate or solute concentration.

Local thickness is an area-weighted metric. It may be an appropriate metric to correlate with mechanical properties, as volume-weighted mechanical property averages are frequently used to predict bulk properties of simple composites.⁸ It may not be difficult to attempt to correlate a bimodal microstructure's thickness mean to its mechanical properties and compare this with a correlation based on its mean lineal intercept.

Mathematical definitions of each grain size metric's probability density function could be explored for regular polygons, which would likely better approximate Voronoi cells or grains than would circles. This would be particularly helpful for applying common stereological ideas to local thickness.

6. References

1. ASTM E112-13. Standard test methods for determining average grain size. ASTM International; 2013. p. 1–28. <https://doi.org/10.1520/E0112-13>.
2. Sosa JM, Huber DE, Welk B, Fraser HL. Development and application of MIPAR: a novel software package for two- and three-dimensional microstructural characterization. *Integr Mater Manuf Innov*. 2014;3:123–140. <https://doi.org/10.1186/2193-9772-3-10>.
3. Russ JC, Dehoff RT. Practical stereology. Springer; 2000. <https://doi.org/10.1007/978-1-4615-1233-2>.
4. Dougherty R, Kunzelmann K-H. Computing local thickness of 3D structures with ImageJ. *Microsc Microanal*. 2007;13:227. <https://doi.org/10.1017/s1431927607074430>.
5. Aurenhammer F. Voronoi diagrams—a survey of a fundamental geometric data structure. *ACM Comput Surv*. 1991;23:345–405. <https://doi.org/10.1145/116873.116880>.
6. Brasz F. Voronoi diagram generator (accessed 2021 Aug 3). <http://cfbrasz.github.io/Voronoi.html>.
7. Fortune S. A sweepline algorithm for Voronoi diagrams. *Algorithmica*. 1987;2:153–174. <https://doi.org/10.1007/BF01840357>.
8. Callister WD Jr, Rethwisch DG. *Materials science and engineering*. Wiley & Sons; 2011.

List of Symbols, Abbreviations, and Acronyms

1D	one-dimensional
2D	two-dimensional
3D	three-dimensional
HTML	HyperText Markup Language
KDE	kernel density estimation

1 DEFENSE TECHNICAL
(PDF) INFORMATION CTR
DTIC OCA

1 DEVCOM ARL
(PDF) FCDD RLD DCI
TECH LIB

2 DEVCOM ARL
(PDF) FCDD RLW MF
B BUTLER
J PARAMORE

1 IOWA STATE UNIVERSITY
(PDF) B KAMAN

1 TEXAS A&M UNIVERSITY
(PDF) D LEWIS